Universiteit Utrecht

Opleiding Natuur- en Sterrenkunde

Measurement of the semi-volatile component of Dissolved Organic Matter in Snow from the Alps by Thermal Desorption-Proton Transfer Reaction-Time of Flight- Mass Spectrometry

BACHELOR THESIS

Arno van den Berg

Supervisors:

Dr. D MATERIC
Marine and Atmospheric Research Utrecht (IMAU)

Prof. Dr. R. HOLZINGER
Marine and Atmospheric Research Utrecht (IMAU)

January 17, 2018

Abstract

Aerosols are small liquid or solid particles suspended in air or gas, or in this case in the atmosphere. Aerosols have a significant impact on climate and are one of the main causes of uncertainty in climate models. Snow samples were collected from the Austrian alps from Febrary 8 until March 18, 2017 to research dissolved organic matter (DOM) originating from deposition of atmospheric aerosols. In this study a novel method was further developed to study DOM using Proton Transfer Reaction-Mass Spectrometry in combination with thermal desorption. The measurements were done at different settings to be able to get nuanced results and to further develop the method. The concentrations found were linked with available meteorological data. The results show that the concentration of organic matter increases in periods with no snow and decreases sharply with fresh snow. A positive correlation was also found between atmospheric pressure and concentration of organic material. Especially pinonic acid and some related ions showed clear correlations.

Contents

1   Introduction

1.1   Aerosols

Aerosols are small, liquid or solid, particles suspended in air. The size of these particles ranges from 10^-3 up to 1 μm for fine and ultrafine particles to about 10-100 μm for coarse particles [9]. These coarse particles generally originate from mechanical action of the wind on the earths surface, whereas the fine particles of less than 1 μm are formed by condensation of precursor gases such as H_2SO_4 [10].

Atmospheric aerosols are also divided into primary and secondary aerosols. Examples of primary aerosols are ash, dust from erosion, or sea salt emitted from the ocean surface, which are often coarse particles. These are all emitted directly at the source, in contrast to secondary aerosols that result from chemical reactions [2]. Other examples of primary aerosols are particles emitted from biomass burning, fossil fuel combustion or volcano eruption. A common marker for biomass burning is levoglucosan, m/z 97.028 [3].

Secondary aerosols, which are usually fine particles, are formed by chemical reactions in the atmosphere. A typical example of this is sulfur dioxide, which is a product of particles coming from fossil fuel combustion. This reacts with water to form gaseous sulfuric acid which in turn will in turn condense to form aqueous sulfate particles which is a fine aerosol. Many other gases condense in the same way to form aerosol [10].

An important part of aerosols is secondary organic aerosols (SOA), which are organic particles formed as oxidation products of volatile organic compounds (VOCs). VOCs are organic compounds that easily change between liquid and gas form. Some of these VOCs are monoterpenes which are emitted from vegetation such as conifers or oaks. Some studies give a yield of 30 percent of VOCs coming from monoterpenes [1]. One oxidation product of monoterpenes that is looked at in this study is pinonic acid. Another important contribution to VOCs is Isoprene, which is emitted from plant foliage. About 38 percent of VOCs is made up of isoprene and its products [6]. According to another study the global amount of isoprene emitted per year is estimated at about 400 to 700 Tg or 440 to 660 Tg carbon.[5].

Aerosols scatter radiation, so most aerosols produce a net negative radiative forcing. In other words, they have a cooling effect [15]. Besides this direct radiative forcing, aerosols also affect the radiation budget indirectly, through their role in cloud formation. They increase the concentration of droplets and decrease the precipitation efficiency and so increase the lifetime of clouds. In other words, they increase the reflectivity of clouds and the overall amount of clouds [14]. Both directly and indirectly, they have a significant effect on the Earths radiation budget.

One of the main sources of uncertainty in climate models is due to aerosols. Climate change and warming due to greenhouse gases has been thoroughly researched and is well known and understood. The effects of perturbations due to greenhouse gases can be modeled fairly easily, but this is more difficult for aerosols [2].

The reason aerosols cause so much uncertainty is because they have much shorter lifetimes than (greenhouse) gases, usually in the order of weeks for the fine and ultrafine particles, or even as short as minutes for some particles [8]. This means that aerosols are not distributed evenly across the globe and stay concentrated close to the source [14]. It is this lack of uniformity that makes it difficult to give much information about aerosols on a global scale.
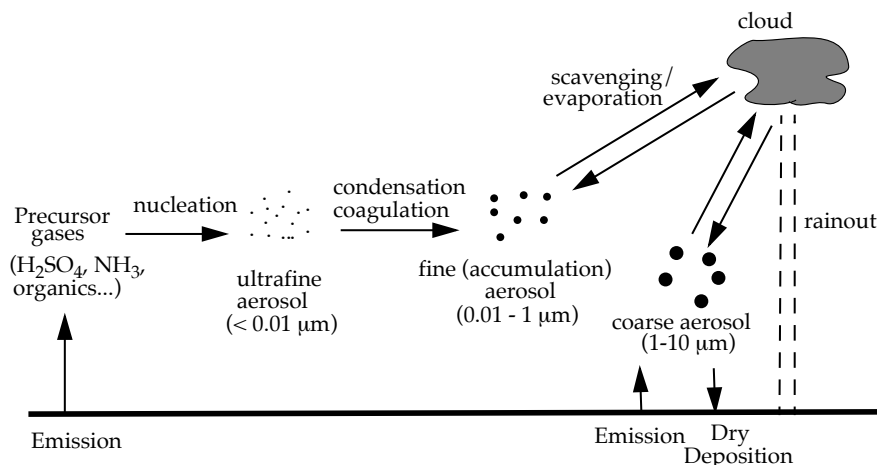
Figure 1: Aerosols and precursor gases are emitted at some source and form into fine and ultrafine aerosols through nucleation and condensation. Coarse aerosols are also emitted due to action of wind on the earth's surface. They are the deposited by wind or rainout. [10]

Typical sinks of aerosols are wet deposition (precipitation), dry deposition (through wind) and sedimentation. At some source precursor gases, such as sulfuric acid and organics, are emitted which nucleate and condense to ultrafine and fine aerosol. Due to their lower mass they can travel longer distances than coarse aerosols before deposition. Coarse aerosol is also emitted due to wind. These aerosols either come back to the surface through dry or wet deposition or are formed into clouds and are then rained out. Figure 1 provides a visual summary of the sources and sinks of aerosols.

1.2   Dissolved Organic Matter in Snow

Of all aerosol particles, the focus in this study is on organic aerosol. This is about a quarter of all fine continental aerosol, though composition varies from place to place due to a lack of uniformity[9]. Snow samples collected from Sonnblick Observatory, in Austria, are measured for dissolved organic aerosol in order to learn more about aerosol composition and travel. Dissolved organic matter (DOM) is an important field of research and many different approaches have been taken to study it. Some widely used methods are fluorescence spectroscopy with excitation emission matrix (EEM) spectroscopy and parallel factor analysis (PARAFAC), as well as UV-Visible spectroscopy. Fluorescence spectroscopy depends on the optically active fraction of DOM, called colored DOM. These particles fluoresce when excited by UV and visible light, especially blue light. This method results in an excitation emission matrix of a series of excitations over multiple wavelengths. PARAFAC is a way to deal with the complex information in EEMs [16].

A novel method is developed by Materić et al [12] to measure DOM from snow samples using Proton Transfer Reaction - Time of Flight - Mass Spectrometry (PTR-ToF-MS). This is a unique method, as PTR-MS only works for gases, not for liquid. PTR-MS is explained further in the material and methods section.

Through deposition and emission, the snow interacts with the atmosphere, and the concentration of aerosol and of DOM in the snow is affected, though not all DOM is originative from aerosols. We linked these measurements with recordings of snowfall and other meteorological data to learn how the concentration of dissolved organic matter coming from atmospheric aerosol is affected. The aim of this study is to learn how the weather affects the concentration of organic compounds found in the snow and to further develop this method for studying DOM.

2   Materials and Methods

2.1   Samples

Snow samples were collected at Sonnblick Observatory in Austria daily from February 8 until March 19, 2017 in the morning between 7:00 and 9:00. Snow was scooped with a sampling flask almost horizontatlly over the surface of the snow, to a depth of about 2 cm. The observatory is located at the top of Mt. Sonnblick, which has a height of 3106 meters above sea level. The mountain is in the main ridge of the Austrian Alps and is one of the highest peaks of the area so it is exposed to winds from all directions. This combination makes this an ideal location to collect samples [4]. The amount of precipitation was also monitored. These samples were kept frozen until the experiment was executed in November 2017.

2.2   Sample Preparation

The snow samples were melted at room temperature and then filtered. The samples were taken with a syringe and then filtered through a 2 μm UNIFLO^{TM} 25/0.2 PTFE filter unit into a 10 ml glass chromatography vial, prebaked at 250 °C. From this vial 1.5 ml was taken with a pipet and transferred into a new 10 ml glass vial. These 1.5 ml samples were capped with a Teflon cap with two 2 mm holes and placed in a desiccator to evaporate at low pressure, after which only semi-volatile organics remained.

To get a low enough pressure, a rotary pump was used and a liquid nitrogen cold trap was placed between the pump and the desiccator to trap the evaporated/sublimated water and backflow of oil vapors from the pump. Typical evaporation time for 1.5 ml samples is about 3 - 4 hours though normally more time was taken to be sure evaporation was complete. See figure 33 for a diagram of the low- pressure evaporation system. After evaporation was complete the desiccator was repressurized gradually by adding nitrogen for about 15 minutes until the desiccator was back at atmospheric pressure. When pressure was restored the vials were removed and the caps were replaced with PTFE caps so that the vials could be measured the following day. The vials and caps were baked overnight at 250 °C before use.

2.3   PTR-ToF-MS

The samples were measured using PTR-ToF-MS, specifically, the PTR-TOF 8000 (IONICON Analytik, Austria). Some of the advantages of PTR-MS are a fast response time, high sensitivity and a low detection limit [11]. VOCs in air are ionized with hydronium ions in the following process:

$$H_3O^+ + M_iH_j \rightarrow M_iH_{j+1}^+ + H_2 \tag{1}$$
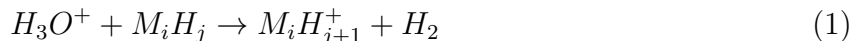
where M is a combination C, O, N and S atoms. H_2O has a proton affinity of 7.22 eV and common organic molecules have proton affinities between 7 and 9 eV, so this reaction is exoergic and quite fast. At the same time, the exoergicity is low enough that there is little break-up of detected neutrals. H_3O^+ is ideal as a proton donor since the most common constituents in air all have electron affinities lower than that of H_2O. In this way, a significant loss of H_3O^+ is avoided. However, some H_3O^+ is lost through the reaction of H_3O^+ with H_2O with any neutral partner to form a complex $H_3O^+H_2O$. This loss is decreased by using
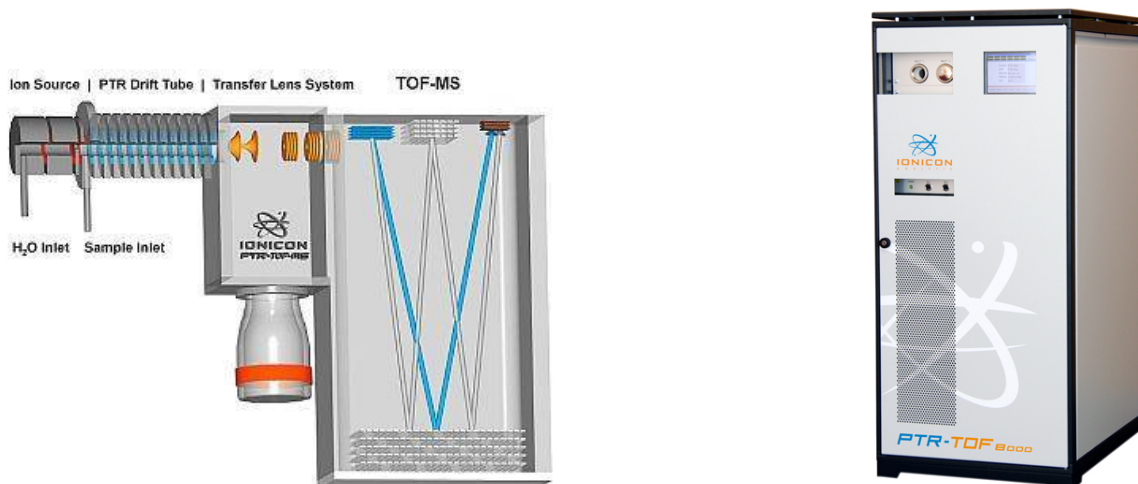
Figure 2: From the website of IONICON: a schematic of PTR-ToF-MS and a picture of the IONICON PTR-TOF 8000 used in this experiment

a high enough E/N (with E being the strength of the electric field and N being the number density of the buffer gas, so E/N is the amount of energy per particle) [7]. In this experiment E/N 120 and E/N 80 were used.

The H_3O^+ ions are produced in a hollow cathode from water vapor. The sample is injected continually in the adjacent drift tube, in which the ionization of the VOCs occurs by the H_3O^+ ions. After these protonated VOCs enter the time-of-flight mass spectrometer via a transfer lens system and are accelerated the flight times are measured, and from this mass to charge ratios, m/z, are determined [11]. See figure 2 for a visualization.

2.4   Thermal Desorption (TD)

In order to measure the samples with the PTR-MS, the sample was heated to release the compounds. The caps of the vials were replaced with caps with two small holes to allow narrow tubes to be placed inside. One tube brings in zero air and the other tube goes to the PTR-MS, which pumps in air. The vials were put in a small oven that fit the vials snugly, which was was heated 40 °C/min to the final temperature of 350 °C, staying at 350 °C for 5 minutes and then cooled down. During this time, the compounds were released (thermally desorbed) and the signal is measured by PTR-MS.

During the TD the samples were flushed with clean air at a rate of around 60 mL/min. Zero air was generated by burning the inflow of ambient air so that no organics from the lab would be read by the PTR-MS. This means extra CO_2 was produced in the zero air generator, but this was not read since the electron affinity is lower than 7.22 eV. The airflow was controlled and at all times there was about 10 ml/min of air more going into the vial than being pumped in by the PTR-MS. The overflow went into the lab. Figure 3 shows a diagram of the TD system. As time and temperature increase during the TD, the amount of molecules registered increases, as can be seen in figure 4 for these particular masses of levoglucosan and pinonic acid, measured in ppb.

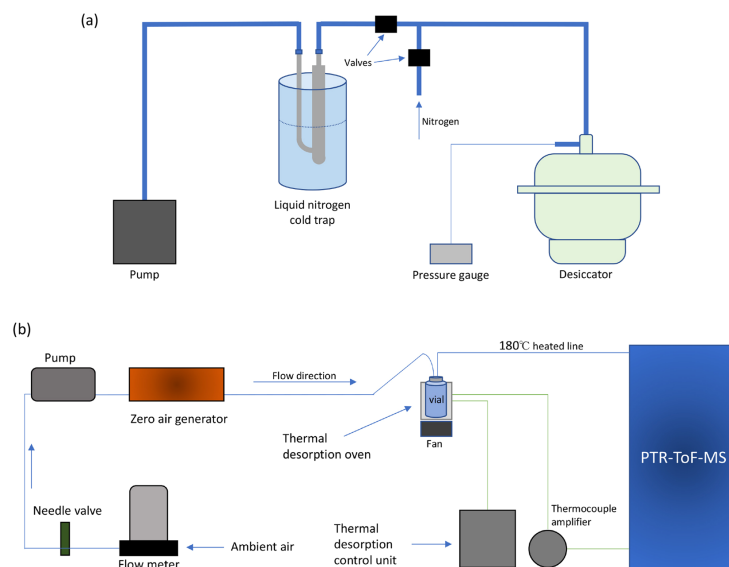Figure 3: (a) Low pressure evaporation system (b) Thermal Desorption system [12]
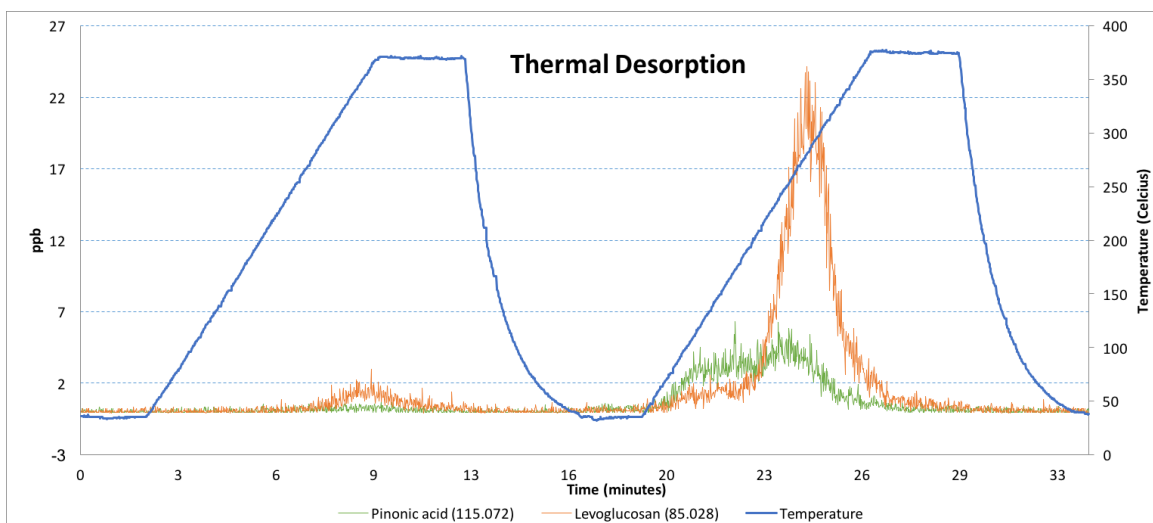

Figure 4: Two thermal desoroption spectra for pinonic acid (green) and levoglucosan (orange). As the temperature increases (the blue line), the amount of these chemicals measured increases and then decreses again as it is close to being completely desorbed. The first desorption is of a blank and the second is of an actual sample.

2.5   Measurement

Each sample was measured in duplicates or triplicates at E/N=120 Td and at 80 Td to allow a robust statistical analysis. However, for some samples there was not enough available for three measurements at each E/N. Priority was given to 120 Td, since this is a standard that balances potential fragmentation and clustering. At 120 Td the velocity of the particles is higher, which results in more fragmentation, and so a higher concentration of hydronium ions and a higher fraction of ionized particles. For the february samples there was not enough time to do three measurements at each E/N. See Table 1 for an overview of all the measurements.

To avoid and assess contamination, several measures were taken. To avoid carryover of compounds that could get stuck in the system during measurement, the measurement of samples was randomized. Also, each day of measurement five field blanks were measured as a background. In addition, three or four system blanks with an empty vial were measured at the beginning of the day to clean the system. The sample preparation was done in such a way as to limit contamination as much as possible, as recommended in the previous work [12].

Depending on which E/N was used, the parameters of the PTR-MS were set as follows. For E/N = 120, the drift voltage (U_{drift}) in the drift tube was set to 600V and for E/N 80 U_{drift} was 400V. Setting the drift voltage affects the reaction time according to the following relation:

$$t \approx \frac{L}{v_d} = \frac{L^2}{\mu U_{drift}} \tag{2}$$

where L is the reaction length, V_d the drift velocity, and μ the mobility of the primary ions H_3O^+ [17]. The temperature of the drift tube was set to 120 °C and the pressure was 3.02 mbar. The Transfer Lens System and the TOF chamber were close to vacuum.

Table 1: Each sample was measured in duplicates or triplicates at both E/N = 120 and E/N = 80. The table shows the dates when the replicas of each sample were measured. Priority was given to E/N = 80 in case there was not enough available for three measurements at each E/N. For the february samples there was not enough time for three measurements at each E/N.

Sample	First replica (120)	Volume	Second replica (120)	Volume	Third replica (120)	Volume	First replica (80)	Volume	Second replica (80)	Volume	Third replica (80)	Volume
8-02-17 0:00	29-11-17	1.5	None	0	None	0	30-11-17	1.5	None	0	None	0
10-02-17 9:00	29-11-17	1.5	None	0	None	0	30-11-17	1.5	None	0	None	0
11-02-17 0:00	29-11-17	1.5	None	0	None	0	30-11-17	1.5	None	0	None	0
12-02-17 8:30	29-11-17	1.5	None	0	None	0	30-11-17	1.5	None	0	None	0
13-02-17 8:05	29-11-17	1.5	None	0	None	0	30-11-17	1.5	None	0	None	0
14-02-17 7:15	29-11-17	1.5	None	0	None	0	None	0	None	0	None	0
15-02-17 8:05	29-11-17	1.5	None	0	None	0	30-11-17	1.5	None	0	None	0
16-02-17 8:05	29-11-17	1.5	None	0	None	0	30-11-17	1.5	None	0	None	0
17-02-17 8:05	29-11-17	1.5	None	0	None	0	30-11-17	1.5	None	0	None	0
18-02-17 7:10	29-11-17	1.5	None	0	None	0	None	1.5	None	0	None	0
20-02-17 8:52	29-11-17	1.5	None	0	None	0	30-11-17	1.5	None	0	None	0
21-02-17 8:52	29-11-17	1.5	None	0	None	0	30-11-17	1.5	None	0	None	0
22-02-17 8:10	29-11-17	1.5	None	0	None	0	30-11-17	1.5	None	0	None	0
23-02-17 8:36	29-11-17	1.5	None	0	None	0	None	0	None	0	None	0
24-02-17 9:00	29-11-17	1.5	None	0	None	0	None	0	None	0	None	0
25-02-17 8:20	29-11-17	1.5	None	0	None	0	30-11-17	1.5	None	0	None	0
26-02-17 0:00	29-11-17	1.5	None	0	None	0	30-11-17	1.5	None	0	None	0
27-02-17 0:00	29-11-17	1.5	None	0	None	0	30-11-17	1.5	None	0	None	0
28-02-17 8:00	29-11-17	1.5	None	0	None	0	30-11-17	1.5	None	0	None	0
2/22/2017 Blank	29-11-17	1.5	None	0	None	0	30-11-17	1.5	None	0	None	0
2/12/2017 Blank	29-11-17	1.5	None	0	None	0	30-11-17	1.5	None	0	None	0
1-03-17 8:33	15-11-17	1.5	16-11-17	1.5	22-11-17	0.75	None	0	None	0	None	0
2-03-17 8:00	15-11-17	1.5	16-11-17	1.5	22-11-17	1.5	None	0	None	0	None	0
3-03-17 8:35	15-11-17	1.5	16-11-17	1.5	22-11-17	1.5	23-11-17	1.5	None	0	None	0
4-03-17 8:00	15-11-17	1.5	16-11-17	1.5	22-11-17	1.5	23-11-17	1.5	None	0	None	0
5-03-17 0:00	15-11-17	1.5	16-11-17	1.5	22-11-17	0.75	None	0	None	0	None	0
6-03-17 8:00	15-11-17	1.5	16-11-17	1.5	22-11-17	1.5	23-11-17	1.5	None	0	None	0
7-03-17 0:00	15-11-17	1.5	16-11-17	1.5	22-11-17	1.5	None	0	None	0	None	0
8-03-17 8:30	15-11-17	1.5	16-11-17	1.5	None	0	None	0	None	0	None	0
9-03-17 8:29	15-11-17	1.5	16-11-17	1.5	22-11-17	1.5	None	0	None	0	None	0
10-03-17 8:20	15-11-17	1.5	16-11-17	1.5	22-11-17	0.5	23-11-17	0.5	None	0	None	0
11-03-17 8:40	15-11-17	1.5	16-11-17	1.5	22-11-17	0.75	None	0	None	0	None	0
12-03-17 8:32	15-11-17	1.5	16-11-17	1.5	22-11-17	1.5	23-11-17	1.5	None	0	None	0
13-03-17 8:40	15-11-17	1.5	16-11-17	1.5	22-11-17	1.5	None	0	None	0	None	0
14-03-17 0:00	15-11-17	1.5	16-11-17	1.5	22-11-17	1.5	23-11-17	1.5	24-11-17	1.5	24-11-17	1.5
15-03-17 8:20	15-11-17	1.5	16-11-17	1.5	22-11-17	1.5	23-11-17	1.5	24-11-17	1.5	24-11-17	1.5
16-03-17 8:00	15-11-17	1.5	16-11-17	1.5	22-11-17	1.5	23-11-17	1.5	24-11-17	1.5	24-11-17	1.5
17-03-17 8:15	15-11-17	1.5	16-11-17	1.5	22-11-17	1.5	23-11-17	1.5	24-11-17	1.5	24-11-17	1.5
18-03-17 8:45	15-11-17	1.5	16-11-17	1.5	22-11-17	1.5	23-11-17	1.5	24-11-17	1.5	None	0
19-03-17 8:36	15-11-17	1.5	16-11-17	1.5	22-11-17	1.5	23-11-17	1.5	24-11-17	1.5	24-11-17	1.5
3/1/2017 Blank	15-11-17	1.5	16-11-17	1.5	22-11-17	1.5	23-11-17	1.5	24-11-17	1.5	24-11-17	1.5
3/8/2017 Blank	15-11-17	1.5	16-11-17	1.5	22-11-17	1.5	23-11-17	1.5	24-11-17	1.5	24-11-17	1.5

2.6   Analysis

Each measurement with the PTR-MS results in a file with a mass spectrum for each temperature step. This was integrated to a file with ppb values for each m/z and the engineering data per complete desorption. With the start and end time of the desorption it was possible to identify each desorption and add the sample date. For each E/N all the blanks were averaged and subtracted from each sample at that E/N. The limit of detection (LOD) was set to two times the standard deviation of all the blanks. Each measurement value that was less than this was set to zero. After this, the ppb values were converted to ng/ml with the following formula:

$$Concentration(ng/ml) = \frac{8 \cdot ppb \cdot M \cdot F}{24.45 \cdot V} \tag{3}$$

with M the molecular mass of the compound, F the flow rate in L/min, and V the volume of the sample loaded in L, times 8 which is the integration time and divided by 24.45 which is the molar volume.

The total concentration of organics was calculated by first excluding all the inorganic compounds and subsequently adding up the total concentration of each compound for each measurement, resulting in up to three values for total concentration. The average of these values was taken and the standard deviation calculated for the error bars if there were two or more measurements.

2.7   Exclusion of outliers

The data showed a few outliers and contaminations. First of all, there were a few outliers in the blanks. For the measurements done on November 22 and 23, 2017, most of the blanks showed exceptionally high values for multiple masses. The values measured for many of the masses on these days were multiple standard deviations higher than the average for all the blanks, so these blanks were excluded from the analysis. Including these blanks would result in much fewer results passing the limit of detection, as more would be subtracted, and the LOD itself would be higher. Normally, the average of the five blanks per measurement day would have been subtracted from the measurements done that same day, but because of these outliers the decision was made to subtract the average of all the blanks from each measurement.

These outliers probably occurred due to some contamination during the sample preparation since the same sample was used for other blanks that did not have such high concentrations. Of the different steps of the sample preparation, the contamination was likely introduced during the preparation of the low pressure evaporation. If the contamination was during filtering it would have shown in all the measurements. During this stage the same pipet was used to transfer 1.5 ml to two or three vials for the low pressure evaporation since they all were extracted from the same vial, so this would have worsened the problem and caused all three blanks to be contaminated.

Another outlier was the sample 10-3. Figure 5 shows the total concentration of organic matter with 10-3 included. As can be seen when compared to Figure 6, the measured concentration of 10-3 is very high. The values for 10-3 are consistently very high, with acceptable error bars, so these high values must be due to the sample itself, and not due to measurement error or contamination during loading. This means the sample was either contaminated during filtering or during collection of the sample, in March. The final possibility is that 10-3 is not an outlier but is actually correct. 10-3 follows the highest amount of snow in the period that is looked at in this study, but this would actually make it more likely that 10-3 is an outlier since the rest of the data shows that a higher amount of fresh snow would predict a lower concentration of organics. For this reason, it was decided to exclude 10-3 from the results.

Finally, the last outliers are one of the measurements of sample 2-3 and one of 11-3 at E/N = 120. In this case something probably went wrong with the measurement or the loading for the low pressure evaporation since it is only one of the three measurements that has an issue. For the 2-3 sample the average of the two normal measurements is 203 while the third measurement is 2600 and for the 11-3 sample the average of the two normal measurements is
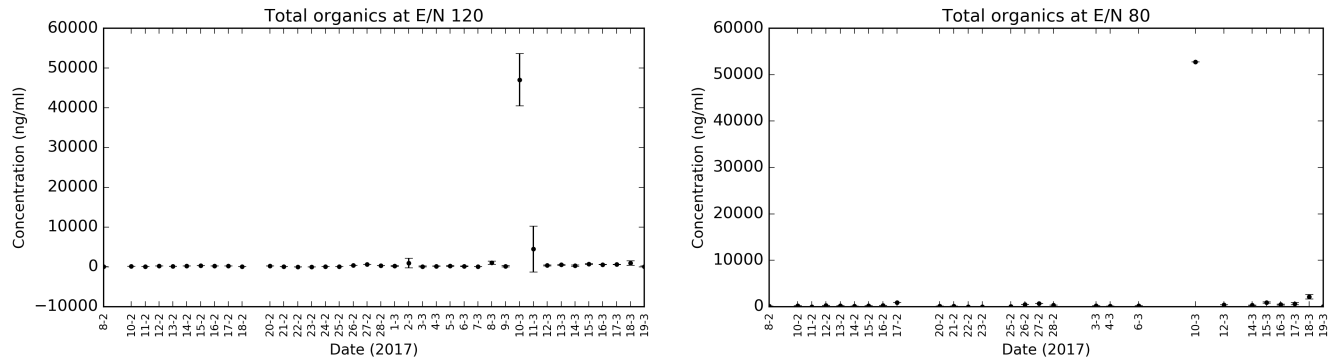
Figure 5: Total concentration of organic matter at E/N = 120 and E/N = 80. Extremely high values are measured for the 10-3 sample constently, so this sample was very likely contaminated, and so is excluded

434 ng/ml while the third measurement is more than 12,000 ng/ml, so these measurements were also excluded.

3   Results and Discussion

In this section the results will be ordered from more general information to more specific compounds. First some information about the total organic mass will be shown and the method will be evaluated. Then some meteorological data will be shown and compared to these results and some data of specific ions and groups of ions.

3.1   Total concentration of organic compounds

The data shows some clear variation over time for the total mass of organics, as can be seen in Figures 6 and 7. At E/N = 120, the plot has peaks on February 27, March 15, and also on March 8 and 18, though with larger error bars. For E/N = 80, the peaks are similar though not exactly the same, as it shows a peak on 17-2 which is not visible in Figure 6.
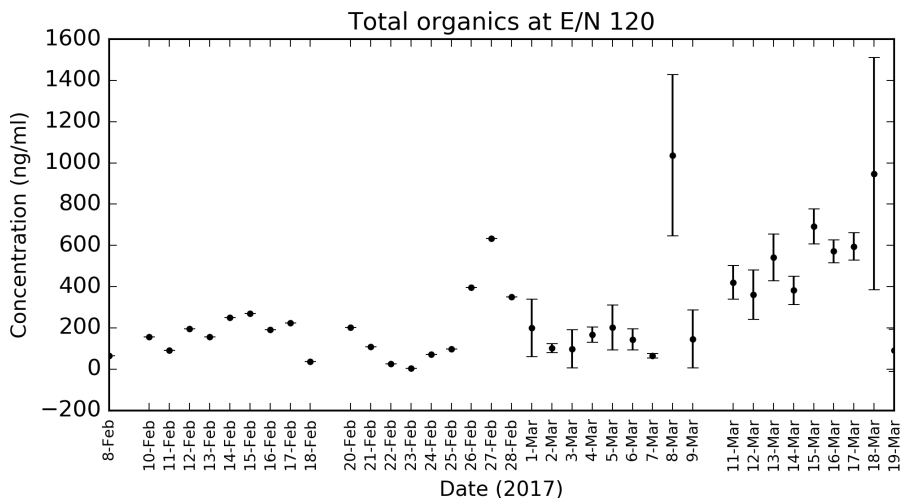

Figure 6: Total concentration of organic mass in snow over time, measured at E/N = 120

Comparing the total concentration of organic mass at each E/N shows that in general the results are fairly equal, though there are a couple results that significantly affect the strength of the correlation. The next plot, Figure 8, shows the total average concentration for both E/N to compare them, with the measurements on E/N = 80 on the vertical axis and E/N=120 on the horizontal axis. The best fit line is given by $y = 1.41x - 13.73$ and the correlation coefficient for this fit is $r^2 = 0.442$, which means the fit matches the data but the correlation is not very strong, though the coefficient could be lower (and better), by excluding samples 17-2 and 18-3 as these are far above the line.

Excluding these two samples would lead to a best fit line of $y = 1.01x + 5.81$ and an R^2 of 0.855. There is no obvious reason to exclude these samples however. 17-2 corresponds to the first peak at E/N 80. The plots of total organic compounds, figures 6 and 7, show that for E/N=80 the peak is at 17-2 whereas for E/N=120 this peak does not show. Also, the peak at 18-3 for E/N = 80 is twice as high as for E/N=120. Because there was only one replica for the 17-2 sample, it is difficult to tell what the root is of this difference. The slope of the best
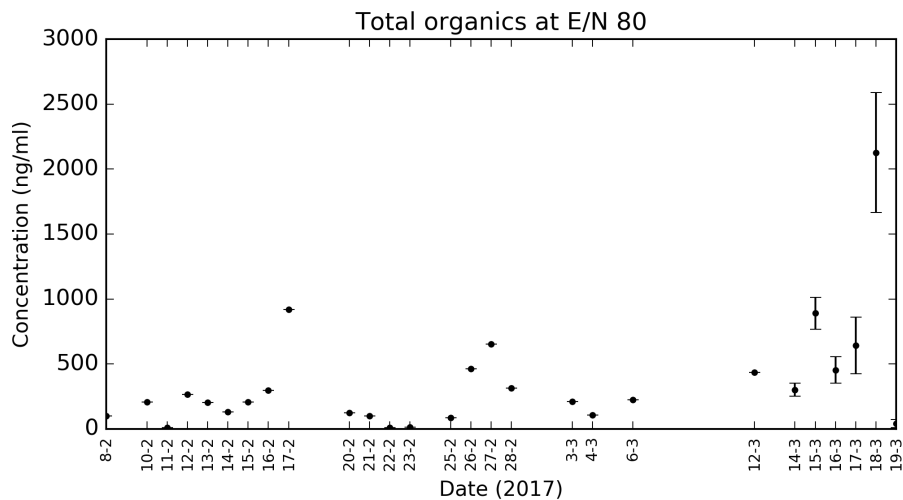
Figure 7: Total concentration of organic mass in snow over time, measured at E/N = 80

fit line is close to 1 with a relatively small negative y-intercept, so the measurements on each E/N are close, though on average at E/N 80 a slightly higher concentration is measured.

There are 14 samples above the dotted line and 12 below this line, meaning that a slightly higher number of samples have a higher measured mass on E/N 80 than on E/N 120. This could be because some compounds have fragmented into smaller compounds at E/N = 120 and not at E/N 80, and have subsequently been excluded because they had a mass smaller than 50 m/z or because the measured mass did not pass the limit of detection.

A similar comparison was done for two specific ions, pinonic acid (m/z 115.072) and levoglucosan (m/z 97.028), which can be seen in figure 9. For pinonic acid the results are very similar at each E/N. The corresponding best fit line is $y = 1.06x - 0.02$ and the correlation coefficient, R^2 is 0.92, which is quite high. The results for levoglucosan do not match as well however. The data is much more spread out and the results are vary more between each E/N. The best fit line is given by $0.57x + 1.02$ and R^2 is 0.39.
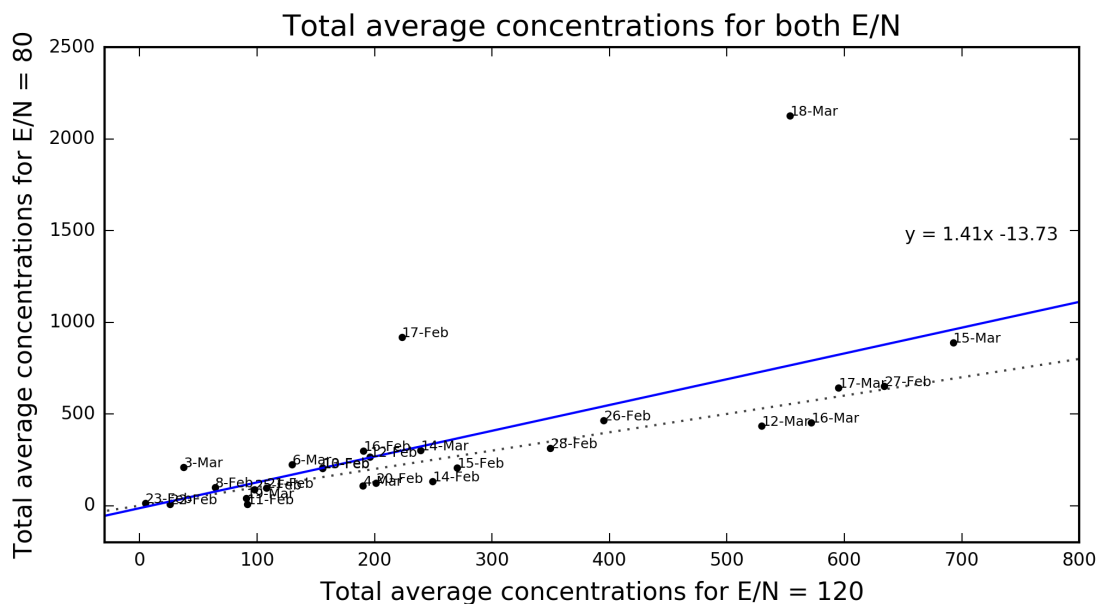
Figure 8: Total average concentration of organics for each E/N. The blue solid line is the best fit line, given by $y = 1.41x - 13.73$ and the dotted line is the line of equal concentrations.
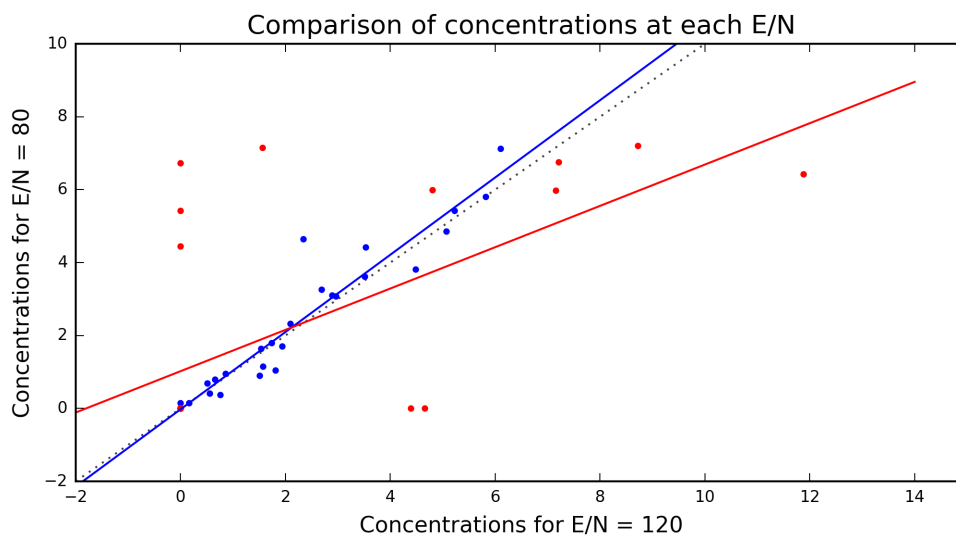

Figure 9: A comparison of the results for pinonic acid, mass 115.072 and levoglucosan, mass 97.028, at each E/N. The blue solid line is the best fit line of pinonic acid, given by $y = 1.06x - 0.02$, the red solid line is the best fit line of levoglucosan, geven by $y = 0.57x + 1.02$ and the dotted line is the line of equal concentrations.

3.2   Relative mass of the compounds

Ions with a higher mass have a greater chance of fragmentation, so it is expected to find more mass in the lower mass ranges, which overall is indeed the case. This can be seen in figure 10 and 11, which shows the relative mass distribution for different mass ranges. Since there should be less fragmentation at 80 Td, it is also expected to find that at E/N = 80 there is a higher concentration of mass measured in higher mass ranges than on E/N = 120. This is the case for most of the samples but not for all.
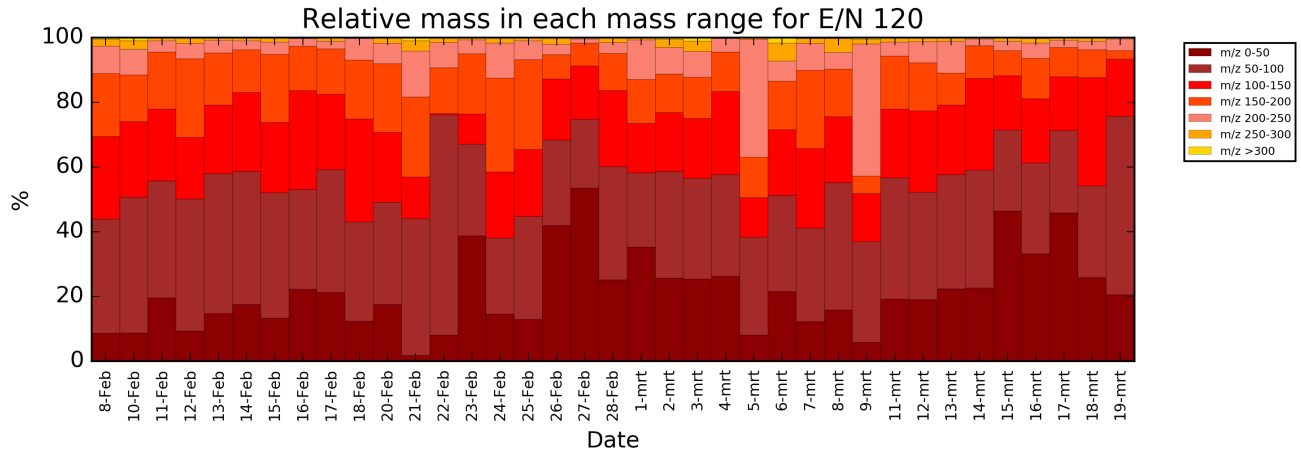

Figure 10: Relative mass in each mass range for E/N = 120
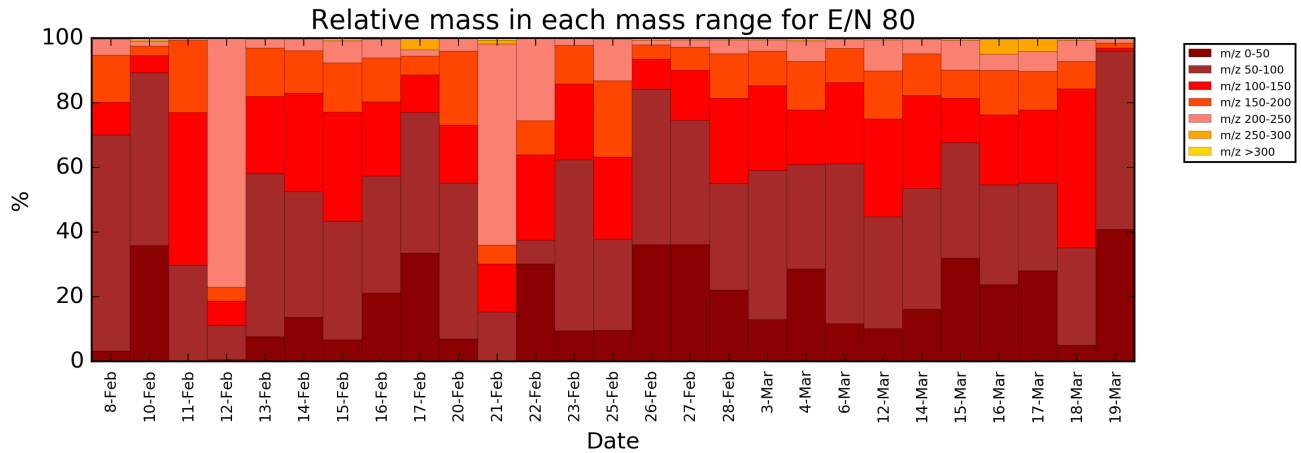
Figure 11: Relative mass in each mass range for E/N = 80

It is interesting that the results are quite different for the different E/N settings. For example, E/N = 120 shows peaks on samples 5-3 and 9-3 for the 200-250 the mass range, whereas for this range E/N = 80 shows peaks on 12-2 and 21-2. These are also exceptions to the expectation to find more mass in the lower mass ranges. It is unclear whether this is the result of a contamination or if something else is going on. The 5-3 sample shows fairly
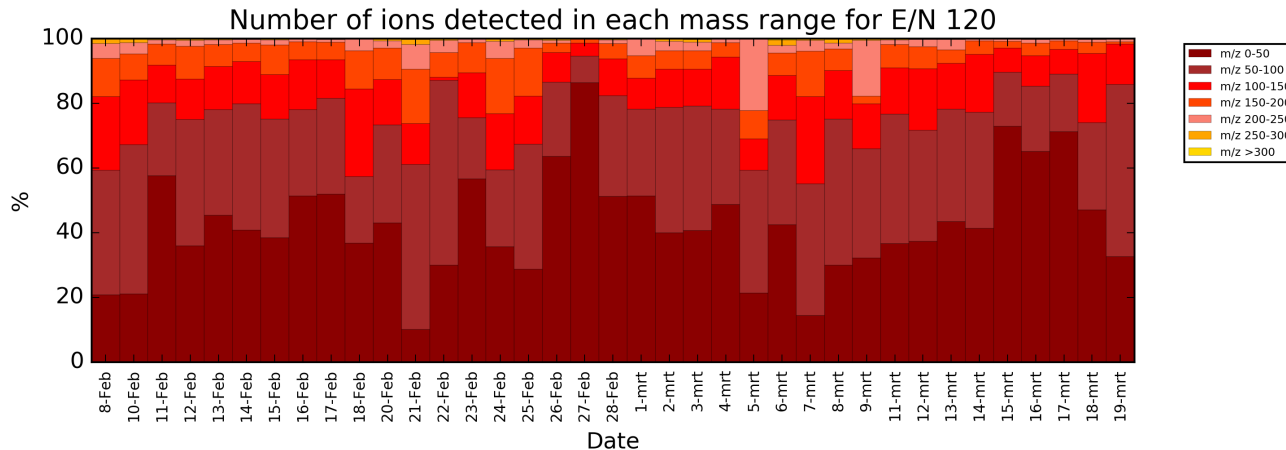
Figure 12: Relative number of ions in each mass range for E/N = 120

Figure 13: Relative mass in each mass range for E/N = 80

little deviation across three measurements but the 9-3 sample does have a higher deviation. For the samples in february there was only one replica which makes analysis more difficult.
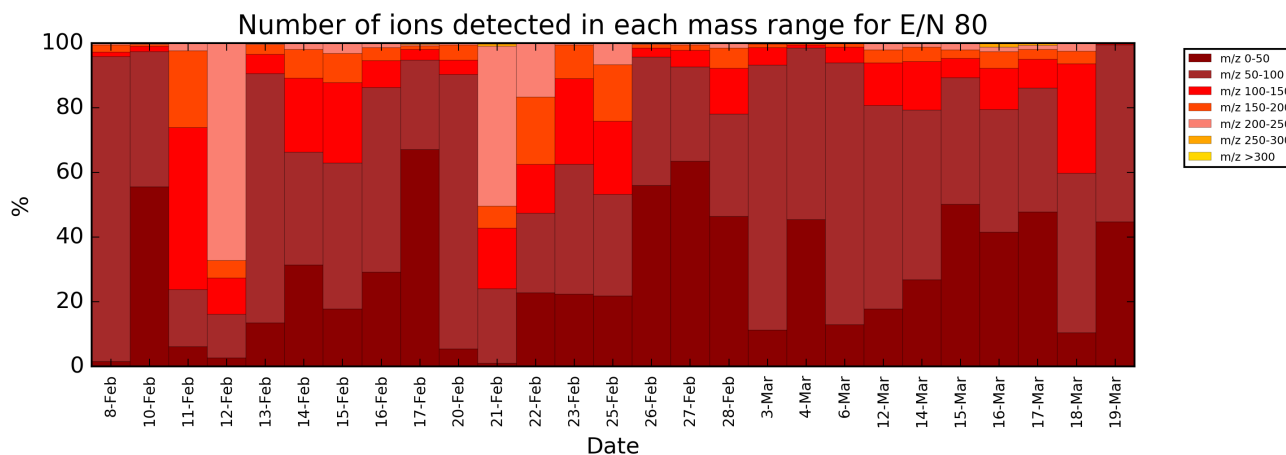
The next figures, figures 12 and 13, show the relative number of ions in each mass range for each E/N. These plots are made from the ppb values after subtraction of the blanks and LOD filtering, but before the conversion to ng/ml. February 12 and 21 are again unique, with a relatively high amount of mass in the higher mass ranges, which is expected since the number of ions and the mass is related. These anomalies warrant further research but that is beyond the scope of this study.

3.3   Meteorological data and mass concentrations

There were some significant variations in the weather over the period that was sampled and it is worth comparing the variation in concentration of organic mass to the variations in the different meteorological data that is available. The concentration can be compared to the

amount of snowfall, wind direction and velocity, humidity, air temperature and atmospheric pressure. Table 2 shows a summary of the total concentration of organic compounds, as was also shown in figures 6 and 7. The table also includes records of snowfall per day and the predominant wind direction, corresponding to figures 14 and 16. Wind direction is given in degrees, with 360 degrees being a Northern wind.

Table 2: Summary of total mass concentration, snowfall, and predominant wind direction. Snow for February 8 is recorded from Feb 7 at 8:01 until Feb 8 at 8:00, and the same for all the following days.

Sample Date	Total concentration of organic compounds at E/N 120 (ng/ml)	Total concentration of organic compounds at E/N 80 (ng/ml)	From	Until	Snow (mm)	Predominant Wind Direction
8-Feb	64.17749804	64.17749804	2/7/17 8:01	2/8/17 8:00	0	NW
7-Feb	No measurement	No measurement	2/8/17 8:01	2/9/17 8:00	0	NE
10-Feb	155.8141147	155.8141147	2/9/17 8:01	2/10/17 8:00	0	SW
11-Feb	91.5212121	91.5212121	2/10/17 8:01	2/11/17 8:00	2	SW
12-Feb	196.1598335	196.1598335	2/11/17 8:01	2/12/17 8:00	0	W
13-Feb	155.6065961	155.6065961	2/12/17 8:01	2/13/17 8:00	0	W
14-Feb	249.4824835	249.4824835	2/13/17 8:01	2/14/17 8:00	0	W
15-Feb	270.3877525	270.3877525	2/14/17 8:01	2/15/17 8:00	0	SE
16-Feb	190.4116768	190.4116768	2/15/17 8:01	2/16/17 8:00	0	S
17-Feb	223.2998279	223.2998279	2/16/17 8:01	2/17/17 8:00	0	NW
18-Feb	35.37576963	No measurement	2/17/17 8:01	2/18/17 8:00	9	N
19-Feb	No measurement	No measurement	2/18/17 8:01	2/19/17 8:00	2.4	N
20-Feb	201.1751154	35.37576963	2/19/17 8:01	2/20/17 8:00	1.6	N
21-Feb	107.8532033	201.1751154	2/20/17 8:01	2/21/17 8:00	1.2	N
22-Feb	25.84456572	107.8532033	2/21/17 8:01	2/22/17 8:00	30.5	W
23-Feb	4.745276485	25.84456572	2/22/17 8:01	2/23/17 8:00	0	W
24-Feb	72.25299492	No measurement	2/23/17 8:01	2/24/17 8:00	4	W
25-Feb	97.55338119	4.745276485	2/24/17 8:01	2/25/17 8:00	9.3	E
26-Feb	394.9783615	72.25299492	2/25/17 8:01	2/26/17 8:00	0	NW
27-Feb	634.1039098	97.55338119	2/26/17 8:01	2/27/17 8:00	0	W
28-Feb	349.5455585	394.9783615	2/27/17 8:01	2/28/17 8:00	0	W
1-Mar	199.5327465	No measurement	2/28/17 8:01	3/1/17 8:00	20.9	NE
2-Mar	953.2390694	No measurement	3/1/17 8:01	3/2/17 8:00	3	W
3-Mar	98.21408527	634.1039098	3/2/17 8:01	3/3/17 8:00	1.3	W
4-Mar	166.993342	349.5455585	3/3/17 8:01	3/4/17 8:00	0	W
5-Mar	202.2163335	No measurement	3/4/17 8:01	3/5/17 8:00	3.1	SW
6-Mar	143.983739	199.5327465	3/5/17 8:01	3/6/17 8:00	7.7	SW
7-Mar	64.81513493	No measurement	3/6/17 8:01	3/7/17 8:00	10.2	N
8-Mar	1036.969111	No measurement	3/7/17 8:01	3/8/17 8:00	12.1	N
9-Mar	146.4030596	No measurement	3/8/17 8:01	3/9/17 8:00	20.3	N
10-Mar	Outlier	Outlier	3/9/17 8:01	3/10/17 8:00	44.9	N
11-Mar	420.6513781	No measurement	3/10/17 8:01	3/11/17 8:00	11.1	NW
12-Mar	360.7200713	98.21408527	3/11/17 8:01	3/12/17 8:00	0	N
13-Mar	541.6739819	No measurement	3/12/17 8:01	3/13/17 8:00	0	N
14-Mar	286.9212866	166.993342	3/13/17 8:01	3/14/17 8:00	0	N
15-Mar	692.670093	202.2163335	3/14/17 8:01	3/15/17 8:00	0	N
16-Mar	571.6285253	143.983739	3/15/17 8:01	3/16/17 8:00	0	N
17-Mar	594.9388965	64.81513493	3/16/17 8:01	3/17/17 8:00	0	N
18-Mar	947.5825684	1036.969111	3/17/17 8:01	3/18/17 8:00	0	NW
19-Mar	90.94452206	146.4030596	3/18/17 8:01	3/19/17 8:00	22.9	NW

3.3.1   Snowfall

When concentration is compared to snowfall, it seems that during periods of snowfall there is a lower concentration of organic mass than during periods of dry deposition, when there is no snowfall. In the period that was sampled, there are several periods of snowfall, with wet deposition of organic aerosol, and several dry periods with dry deposition. Figure 14 shows a few instances where, during a period of no snow, there is a gradual increase in the concentration of organic compound followed by a decrease after the first snow. This happens for the samples for 11-2, 18-2, 22-2, 1-3, and 19-3. This means that during periods of snow there would be less deposition of aerosol.

This trend could make sense because during a period of no fresh snow there is more time for organic compounds to be deposited, whereas new snow may cover this up with a new layer with a lower concentration. On the other hand, the sampling depth is close to 20 mm so not only new snow would be taken. It is worth noting that sample 10-3 showed an exceptionally high concentration, as was discussed in the exclusion of outliers, and that this corresponds with the highest measurement of snowfall. Most of the other peaks of snowfall correspond with dips in the concentration of organics however, which would confirm sample 10-3 being an outlier due to some kind of contamination. A notable exception is that between the snow on 25-2 and 1-3, the peak is on 27-2 and then concentration decreases before the snow comes.
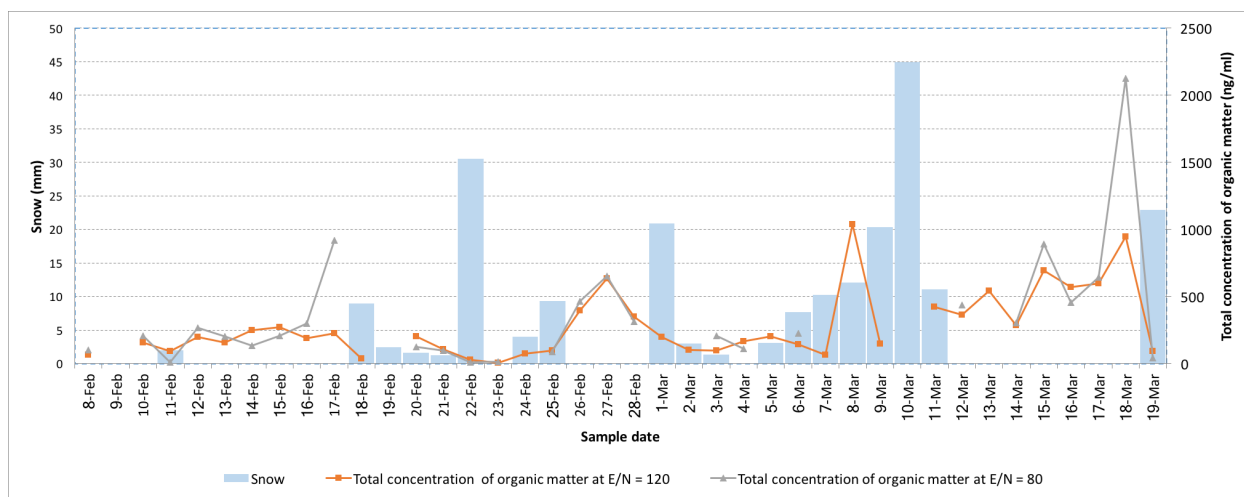

Figure 14: Overview of snowfall and total concentration of organic matter. Snowfall is on the left vertical axis and total concentration is on the right vertical axis. Snowfall is measured from 8:01 the previous day until 8:00 on the day that it shows on this plot.

In order to statistically prove the difference between periods of snow and now snow, a t-test was done for each m/z and at both E/N for concentrations during snow versus no snow. Table 3 shows the ions for which the p-value was less than 0.05 at both E/N. The dataset contained many zeros due to the limit of detection filtering which caused many of the P-values to be unrealistically low. The t-test was done again excluding the zeros. After excluding the zeros, many of the data sets were too small so the t-test was only done for the ions for which there were 5 or more values in both the snow as well as the no snow samples. At E/N = 120 there were 138 ions that had a P-value under 0.05 and at E/N =

80 there were 50. Many of these still had exceptionally low p-values of less than 1% but most of those were for masses where the P-value was under 0.05 only for one of the E/N. For total concentration of organic aerosol, the results seemed to show a correlation between snow and no snow, where during periods of no snow there was an increase in concentration, followed by a decrease when it snowed, which suggests that dry deposition has a larger effect on concentration.

m/z	p-value for E/N =120	p-value for E/N = 80	m/z	p-value for E/N =120	p-value for E/N = 80
67.053	0.00370697	0.032448192	153.091	0.000904408	0.016097182
98.052	0.008657585	0.030293501	153.109	0.00164485	0.01116505
105.055	6.78E-05	0.021401979	165.089	0.004830422	0.029831731
106.054	0.015662308	0.04492183	167.1	0.000555934	0.002841408
113.051	5.56E-05	0.001533562	169.1	0.003806052	0.025342227
114.056	0.000517132	0.031515109	171.099	0.000567821	0.039045333
115.072	6.96E-05	0.014224401	171.12	0.001088409	0.014924605
125.056	0.002631324	0.003566289	172.097	0.000710215	0.032230226
127.072	0.000585593	0.007640845	178.062	0.020220867	0.027989969
128.07	0.000172588	0.020794062	179.099	0.000340142	0.007243469
129.06	0.037403929	0.030944723	181.107	0.00013201	0.003596078
129.076	0.000552213	0.001950819	185.118	0.001474719	0.025876099
133.055	0.000750066	0.022768781	195.125	0.030151508	0.031954777
139.082	0.00066757	0.004790093	198.107	0.02649336	0.047669805
141.082	0.00051124	0.006998408	199.139	0.008664979	0.020336272
142.081	0.001155514	0.022902256	225.129	0.01241488	0.038445998
143.075	0.006072374	0.028176436	231.104	0.032229666	0.04138492
143.104	0.003493107	0.018654752	267.138	0.005655656	0.009656159
151.076	0.012163835	0.012207947			

Table 3: Ions for which the P-values as a result of the t-test are below 0.05 at both E/N

3.3.2   Atmospheric Pressure

Figure 15 shows atmospheric pressure with concentration of organic matter on each E/N. This plot shows clear variation across the samples. Due to the high altitude the pressure is consistently lower than standard atmospheric pressure, but with some clear peaks and drops. The expectation is that an increase in pressure should play a role in deposition of aerosol, namely to cause an increase in deposition, which seems to indeed be the case. Increases in atmospheric pressure seem to correspond with increases in concentration of organic matter, which would match the prediction. There are a few mismatches however, as the peak in concentration on 2-3 precedes the peak in atmospheric pressure, which does not follow the overall trend. Also, the peak for atmospheric pressure is on March 15, whereas the peak for organic matter is a few days later, on March 18.
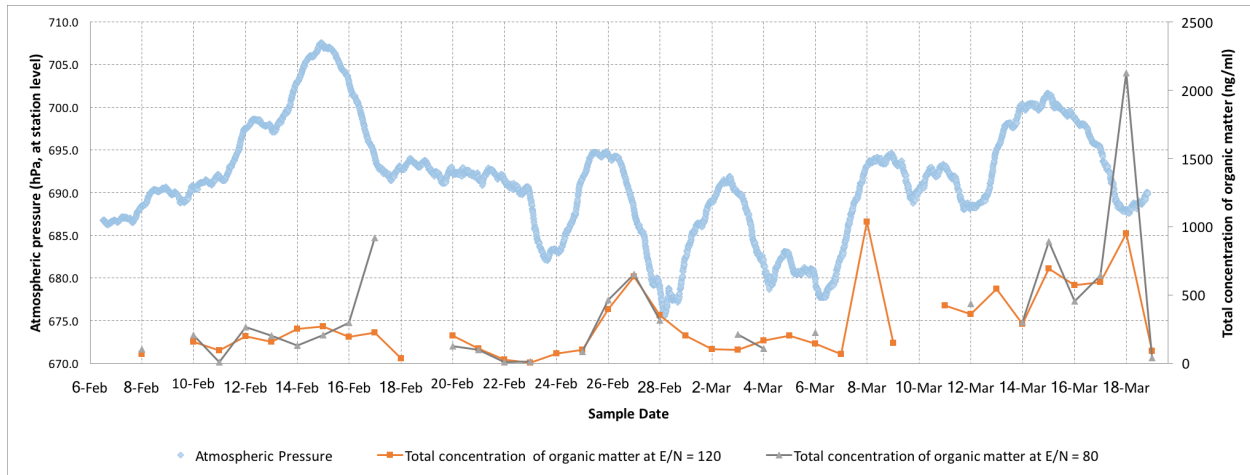
Figure 15: Overview of atmospheric pressure and total concentration of organic matter, with pressure on the left axis and concentration on the right axis.

3.3.3   Wind direction and velocity

Figures 16 and 17 show the wind direction and velocity. Overall the predominant wind direction is Northern. The wind velocity varies both throughout the day as well as across days. February 10-12, 21, 24, 28, March 3-5 and 18 show some extra high wind speeds of above 16 m/s. These are gale force winds, or 8-10 on the Beaufort scale. It is possible that such winds would cause more dry deposition in periods with no snowfall, but this does not seem to be the case looking at these figures.
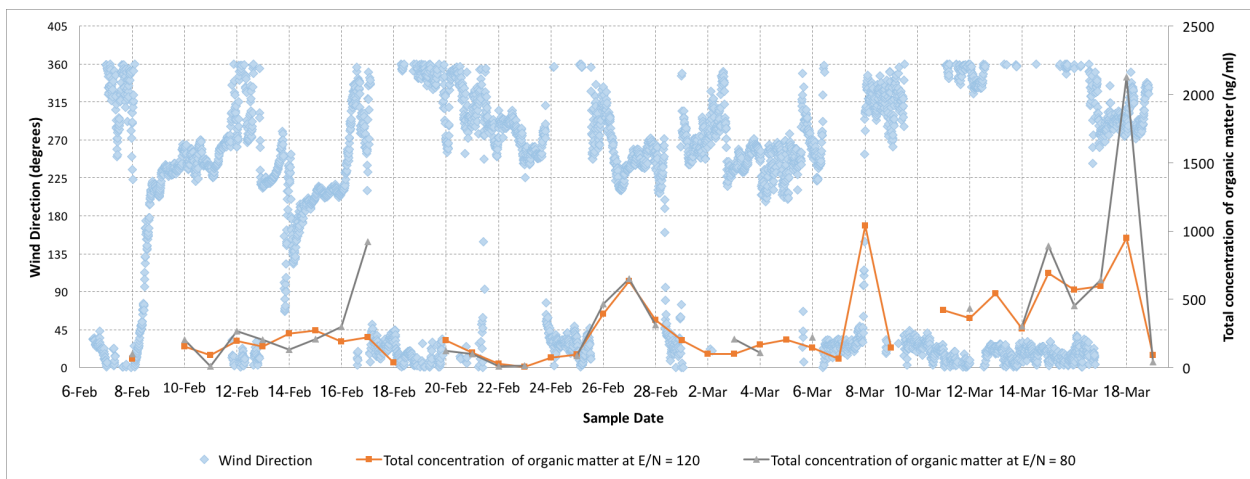

Figure 16: Overview of wind direction and total concentration of organic matter. Wind direction is on the left vertical axis, in degrees, with 360 degrees being a Northern wind and 90 degrees being an Eastern wind. Total concentration is on the right axis.
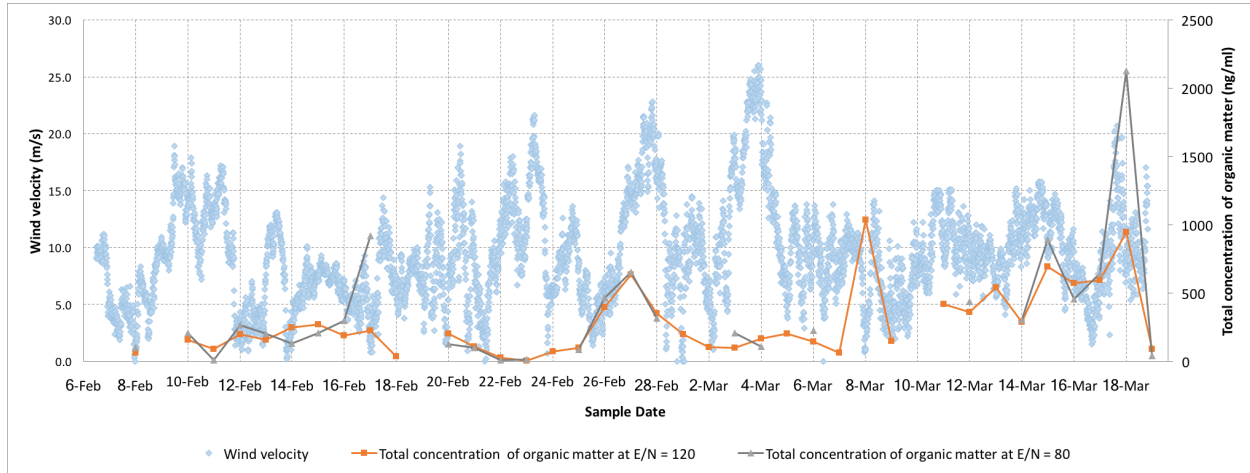
Figure 17: Overview of wind velocity and total concentration of organic matter. Wind velocity is on the left vertical axis, in m/s and total concentration is on the right vertical axis.

3.3.4 Humidity

Related to snowfall is the humidity, which is shown in figure 18. Higher periods of snowfall correspond to higher humidity in this plot. A relation between humidity and concentration of organic mass would probably be due to the same mechanism as the relation of concentration with snowfall. A clear relation cannot be found however.
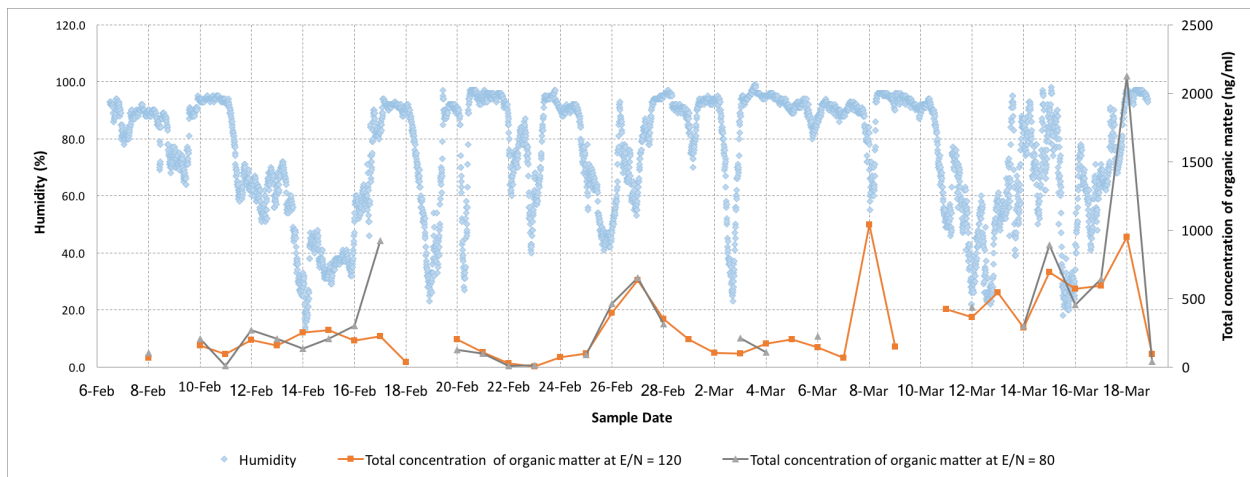

Figure 18: Overview of humidity and total concentration of organic matter. Humidity is on the left vertical axis, in % and total concentration is on the right vertical axis.

3.3.5 Air Temperature

Figure 19 shows the air temperature. There are some significant variations across these few weeks but the temperature consistently stays below zero, so the temperature shouldnt have

a large impact on the concentration of organic compounds. Any impact temperature does have would be positively related to concentration. There are peaks in the temperature on February 14-16, 21-24, 27, a small peak on March 3, March 9, and a general increase to march 18 and 19. Looking at figure 19 it is possible that temperature and concentration are related as can be inferred from the correlation between the peaks around february 27 and 28 and the peak around march 17-18, but the correlation does not continue for the rise in temperature around february 14-16 and february 20-23.
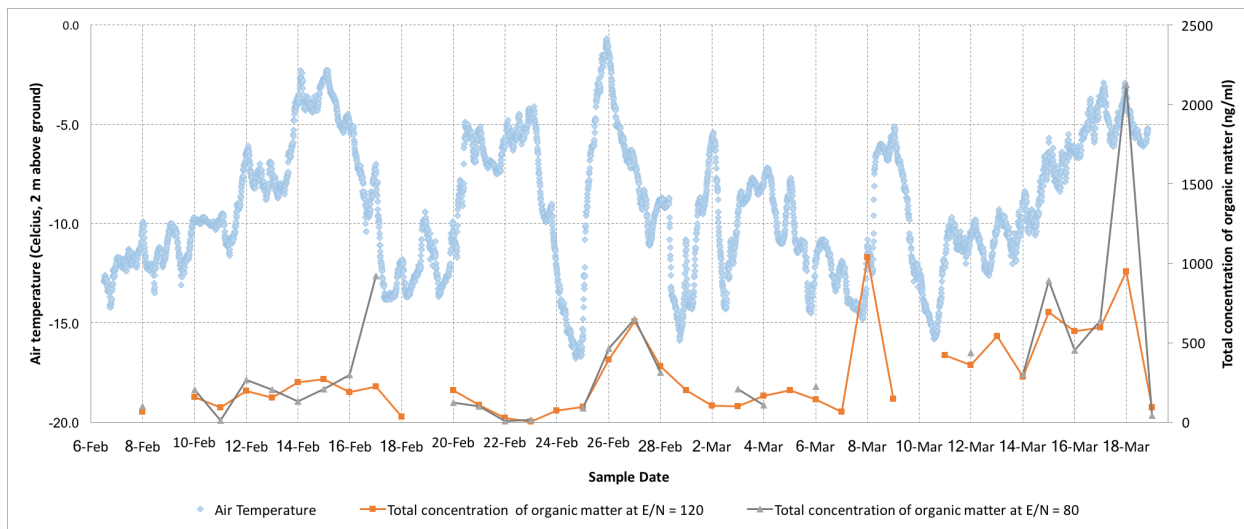

Figure 19: Overview of air temperature in °C, measured 2m above the ground, and total concentration of organic matter.

3.4   Pinonic Acid

A further look at table 3 with the the ions that show a significant difference between snowy and dry periods, shows that many of the the ions for which the P-value was less than 0.05 for both E/N have a similar shape, corresponding to the shape of the plot of pinonic acid, mass 115.072. Pinonic acid is an oxidation product of monoterpenes, which are emitted from vegetation, the plot of which can be seen in figure 20. The plots of these ions have peaks at 16-2, 27-2, and a general increase to a peak at 18-3. There are also several smaller peaks in between that are also mostly similar for these plots. Table 4 shows the ions that have a correlation coefficient, R^2 higher than 0.6 when compared to pinonic acid.

The correlation between snowfall and the behavior of pinonic acid is even more clear than for the total concentration of organic matter. This can be seen in figure 21. When compared to atmospheric pressure, seen in figure 22, the results are also clearer than those for total concentration. There seems to be quite a clear correspondence between pressure and concentration.

The list of ions with similar behavior to pinonic acid is quite long, with 221 ions with an R^2 coefficient higher than 0.6, and the behavior of pionic acid is fairly similar to that of the total concentration, seen in figures 6 and 7, which suggests that the total concentration of organic compounds is strongly dependent on these ions that are similar to pinonic acid.
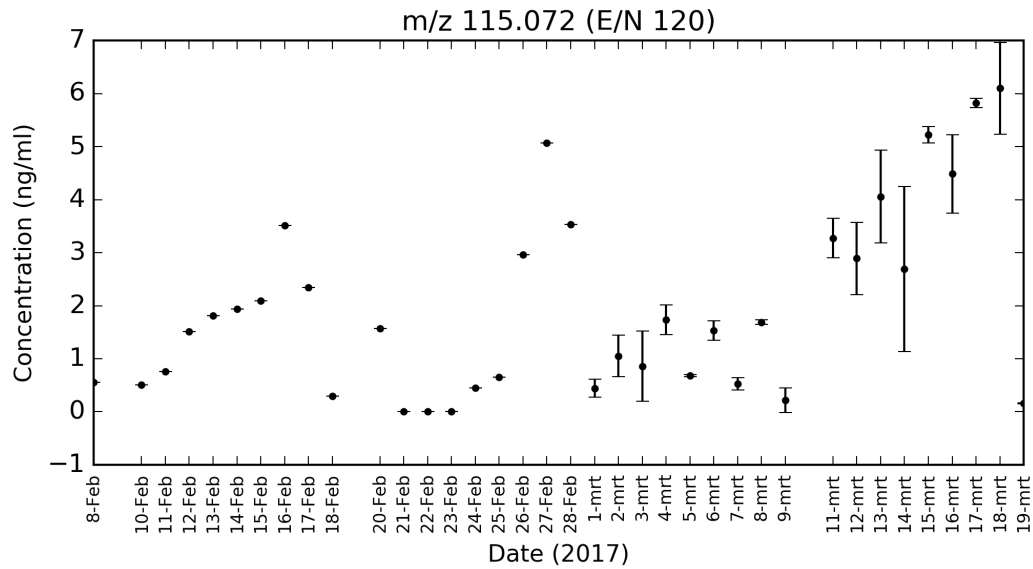
Figure 20: Plot of concentration of pinonic acid, mass 115.072
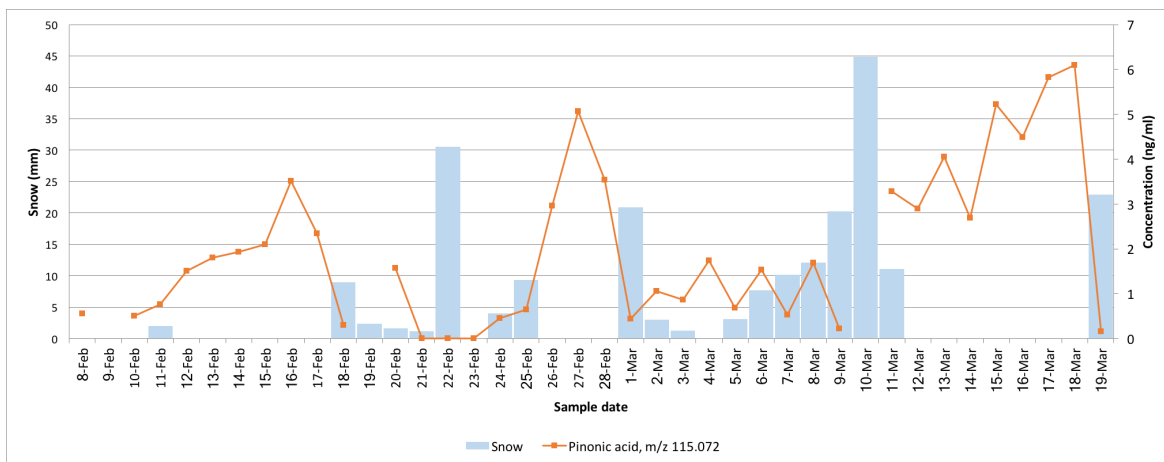

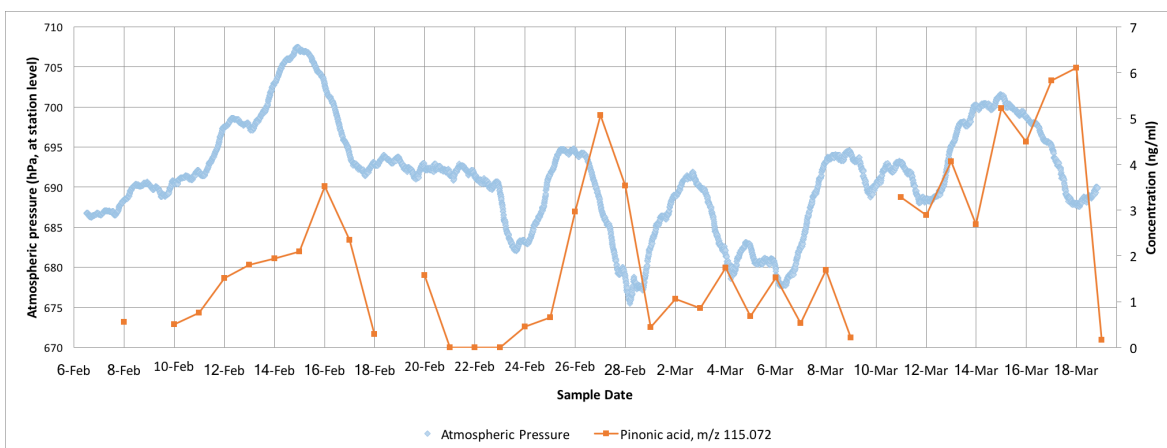Figure 21: Overview of snowfall and concentration of pinonic acid

Figure 22: Overview of atmospheric pressure and concentration of pinonic acid

Table 4: The ions that have a similar shape to pinonic acid, m/z 115.072, with the corresponding R^2. Only the ions are shown for which R^2 is higher than 0.6.

m/z	R-squared	m/z	R-squared	m/z	R-squared	m/z	R-squared	m/z	R-squared	m/z	R-squared
15.022	0.627259588	88.072	0.817055724	127.072	0.970668457	159.974	0.6011916	186.097	0.68358989	217.042	0.805908248
29.997	0.718230314	89.042	0.623785187	128.049	0.691442737	161.065	0.825667348	187.071	0.696685515	217.089	0.839819787
30.995	0.733651506	89.056	0.655616394	128.07	0.930089486	161.078	0.737266866	187.1	0.775509943	218.09	0.700125064
31.018	0.748221715	90.021	0.734713469	129.06	0.895705533	162.059	0.724567015	188.076	0.739957548	218.106	0.881911548
41.038	0.778234205	90.054	0.825746392	129.076	0.946177596	162.071	0.775965734	188.107	0.783262332	219.057	0.791293511
43.018	0.727400778	95.055	0.723300203	130.057	0.848197625	163.054	0.783628945	189.072	0.895554612	219.101	0.775395815
43.053	0.765433469	96.044	0.910421604	132.069	0.601899132	163.093	0.775365489	190.066	0.860876556	219.12	0.728322464
46.028	0.65137194	97.055	0.794711047	133.055	0.845886484	164.053	0.843405958	191.07	0.910468392	220.092	0.803301918
47.023	0.61459656	98.026	0.821850861	134.058	0.834309387	164.064	0.910100718	191.102	0.915074757	221.108	0.784049736
48.009	0.781305936	98.052	0.914484309	136.07	0.70809369	165.04	0.844921229	195.112	0.659662767	222.106	0.747349743
49.028	0.757925806	99.01	0.788066169	137.062	0.608625484	165.089	0.913490868	196.099	0.779465034	225.129	0.672145978
53.036	0.627483014	99.045	0.872821931	139.082	0.959319516	166.064	0.724351976	196.13	0.733998611	229.022	0.643443224
61.028	0.650977458	102.088	0.690260924	140.063	0.879701767	166.092	0.851767879	197.119	0.850749258	230.099	0.79748983
62.026	0.638609917	103.04	0.7129293	141.082	0.961414687	167.1	0.960322595	197.133	0.830007916	231.087	0.822331774
63.021	0.614982007	105.055	0.620787136	142.05	0.889557027	168.099	0.924071419	198.107	0.851996212	232.101	0.829742037
64.041	0.685419784	107.053	0.60095149	142.081	0.933609268	169.1	0.917301051	198.128	0.853199773	233.118	0.673780532
66.021	0.668042165	108.048	0.839598938	143.075	0.894980779	171.042	0.719601829	199.111	0.851170091	235.132	0.865766595
67.041	0.733377722	108.078	0.775237475	143.104	0.793962092	171.099	0.917224241	199.139	0.616109204	235.174	0.75473833
67.053	0.887298516	109.054	0.861421637	143.964	0.646478963	171.12	0.799713453	200.091	0.60941983	236.112	0.787584446
68.049	0.753485568	109.097	0.856151559	144.068	0.872586584	172.097	0.88226706	200.109	0.866017444	241.088	0.68788065
69.068	0.808295275	110.059	0.909217747	145.066	0.818780157	172.956	0.65350251	202.089	0.799400715	241.134	0.788058544
70.031	0.840140277	110.081	0.860075373	146.061	0.807409616	173.082	0.831385799	202.136	0.814360866	242.141	0.638583136
70.065	0.773107295	112.049	0.891451779	147.051	0.652926826	173.141	0.826824584	203.078	0.863319493	246.089	0.709867016
71.048	0.896673745	112.071	0.826072391	151.076	0.690717381	177.074	0.803569773	203.093	0.844304123	247.109	0.77663131
72.046	0.800579331	113.038	0.719856381	152.08	0.860375157	179.085	0.841336144	204.089	0.906065823	247.156	0.677791301
80.039	0.711971391	113.051	0.948931777	153.091	0.932470919	179.099	0.843182161	205.095	0.83430821	251.146	0.704684023
81.035	0.699638554	114.044	0.892173658	153.109	0.905362792	180.082	0.899233218	205.121	0.754981866	253.161	0.685346195
82.038	0.854676243	114.056	0.708983267	154.084	0.728634944	181.083	0.861719003	206.081	0.847200849	255.141	0.765873981
82.064	0.728348059	114.088	0.762245809	154.097	0.938653102	181.107	0.94133288	209.152	0.751267977	259.131	0.770736761
83.048	0.762171848	115.041	0.837659246	155.086	0.81350443	182.08	0.772196844	210.131	0.694142227	261.144	0.632921965
84.045	0.83462195	116.041	0.880398564	155.097	0.94360544	182.097	0.934956107	211.123	0.855005825	263.126	0.763090609
85.061	0.863219813	116.07	0.940954962	156.083	0.926753475	183.102	0.924497344	212.123	0.847665394	263.146	0.719963154
86.029	0.68973435	117.055	0.768699254	157.068	0.888034376	184.088	0.814019975	214.092	0.711754597	265.145	0.789338635
86.059	0.831259625	120.05	0.630765114	157.084	0.617747672	184.119	0.615124658	215.071	0.731314165	271.151	0.678734212
87.043	0.886896544	124.044	0.880221099	157.113	0.878196283	185.118	0.940177301	215.104	0.829190469	273.139	0.747646325
88.041	0.731539548	125.056	0.934110034	158.069	0.805023649	185.167	0.642602644	215.191	0.681725643	275.133	0.677574795
		126.055	0.813796857	158.095	0.83011729	186.065	0.663898007	216.097	0.864850617	277.141	0.615084271

3.5   Levoglucosan

Another group of ions corresponds to the behavior of levoglucosan. See table 5 for an overview of the ions that show this behavior, with their respective R^2 values. Only the ions with an R^2 higher than 0.6 are shown. Levoglucosan shows significantly different behavior from pinonic acid and total concentration, which can be seein in figure 23 in the plot of levoglucosan. All these ions show very little or no activity until March 6 and then increase to a peak at March 18. As levoglucosan is a marker for biomass burning it is interesting to find out where these ions may have come from and what changed after March 6.

The predominant wind direction during this period from March 6 until 18 was Northern, as can be seen in table 2 so these molecules would come from the direction of Germany and possibly from Salzburg and Munich. However, this should not be the cause of the increase in levoglucosan as there were also other times with Northern winds during the period that was sampled.
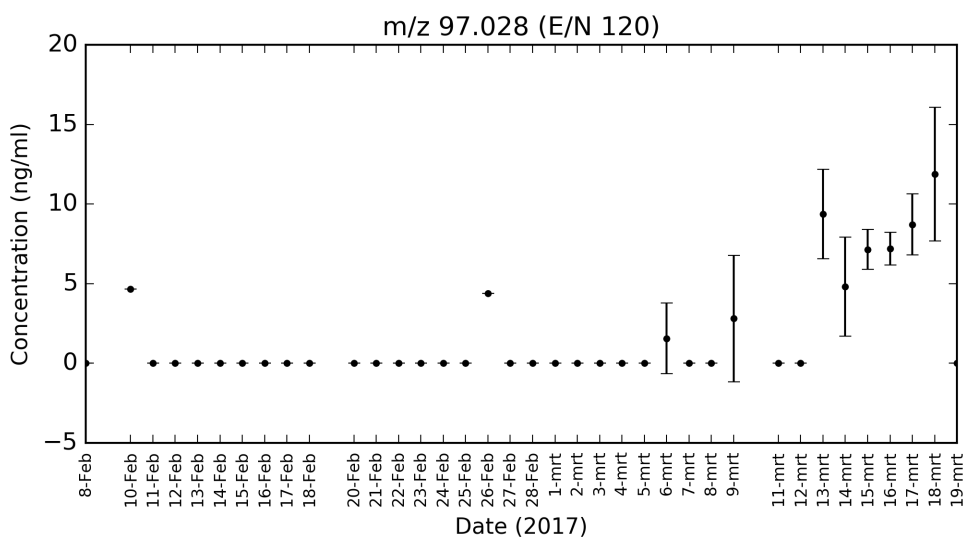

Figure 23: Plot of the concentration of levoglucosan, mass 97.028

Table 5: The ions that have a similar shape to levoglucosan, m/z 97.028, with the corresponding R^2. Only the ions are shown for which R^2 is higher than 0.6.

m/z	R-squared	m/z	R-squared	m/z	R-squared	m/z	R-squared	m/z	R-squared
53.036	0.76081874	85.028	0.918992161	113.038	0.630491	113.038	0.630491	128.049	0.798593
60.079	0.61456935	86.029	0.65058306	125.026	0.883908	125.026	0.883908	145.056	0.786032
69.034	0.9303137	99.045	0.698747508	125.958	0.678954	125.958	0.678954	145.066	0.668823
83.048	0.67287004	103.04	0.637765181	127.04	0.843024	127.04	0.843024	146.061	0.646784
84.045	0.64190703	109.029	0.920597978	127.946	0.607588	127.946	0.607588	159.974	0.61787

4   Conclusion

The total concentration of organic compounds measured with the PTR-MS varies between about 5 ng/mL on February 23 and 1 μg/ml on March 2, 8 and 18, with another slightly lower peak on February 27 for E/N = 120. At E/N = 80 there is also a peak on February 17 and the peak at March 18 is significantly higher than at E/N = 80. These two values are what cause the best fit line to be more on the side of E/N = 80. Besides these two values, however, the rest of the measurements are grouped around the line of equal concentrations. Overall the conclusion can be made that both the E/N = 120 and E/N = 80 give close to the same results, though slightly higher amounts are measured at E/N = 80 due to some more fragmentation at E/N = 120. Because of these differences it is recommended to continue using both E/N settings to be able to compare the results.

Linking total concentration of organic compounds to the meteorological data shows that during periods of no snow and dry deposition the concentration of organic material in the snow increases significantly, and then decreases with a new layer of snow. Fresh snow does have some concentration of organic compounds, but dry deposition adds more to the total concentration. The total concentration also corresponds positively to atmospheric pressure.

For pinonic acid, and the long list of other ions that have similar behavior, the results are more clearly related to snowfall and atmospheric pressure. During the periods with no snow there is a very clear increase in concentration and a very clear decrease during the snow. Increases in atmospheric pressure are also clearly followed by increases in concentration of pinonic acid.

It is yet unclear whether the variation is directly or indirectly dependent on the weather. It could be that the weather affects aerosol formation in the atmosphere or aerosol deposition. From the correlation with snow, the variation is more likely based on deposition.

Further research could take a more in depth look into the different ions that show the same behavior and what the cause could be.

References

[1] Barthelmie, R. J., and PryorS. C. 1999. "A model mechanism to describe oxidation of monoterpenes leading to secondary organic aerosol: 1. pinene and pinene." *Journal of Geophysical Research: Atmospheres* 104 (D19): 23657-23699.

[2] Boucher, O., D. Randall, P. Artaxo, C. Bretherton, G. Feingold, P. Forster, V.-M. Kerminen, et al. 2013. "Clouds and Aerosols." In *Climate Change 2013: The Physical Science Basis. Contribution of Working Group I to the Fifth Assessment Report of the Intergovernmental Panel on Climate Change*, by T.F., D. Qin, G.-K. Plattner, M. Tignor, S.K. Allen, J. Boschung, A. Nauels, Y. Xia, V. Bex and P.M. Midgley Stocker. Cambridge: Cambridge University Press.

[3] Fraser, M.P., and K. Lakshmanan. 2000. "Using levoglucosan as a molecular marker for the long-range transport of biomass combustion aerosols." *Environmental Science & Technology* 34 (21): 4560-4564.

[4] Grllert, C., A. Kasper, and H. Puxbaum. 1997. "Organic Compounds in High Alpine Snow." *International Journal of Environmental Analytical Chemistry* 67:1-4: 213-222.

[5] Guenther, C. C. "Estimates of global terrestrial isoprene emissions using MEGAN (Model of Emissions of Gases and Aerosols from Nature)." *Atmospheric Chemistry and Physics* 6 (2006).

[6] Hallquist, Mattias, J. C. Wenger, Urs Baltensperger, Y. Rudich, David Simpson, M. Claeys, J. Dommen, and et al. 2009. "The formation, properties and impact of secondary organic aerosol: current and emerging issues." *Atmospheric Chemistry and Physics* 9 (14): 5155-5236.

[7] Hansel, A., A. Jordan, R. Holzinger, P. Prazeller, W Vogel, and W Lindinger. 1995. "Proton transfer reaction mass spectrometry: on-line trace gas analysis at the ppb level." *International Journal of Mass Spectrometry and Ion Processes* 149: 609-619.

[8] Haywood, J., and O. Boucher. 2000. "Estimates of the direct and indirect radiative forcing due to tropospheric aerosols: A review." *Reviews of geophysics* 38 (4): 513-543.

[9] Heintzenberg, Jost. 1989. "Fine particles in the global troposphere A review." *Tellus B: Chemical and Physical Meteorology* 41 (no. 2): 149-160.

[10] Jacob, Daniel J. 1999. *Introduction to Atmospheric Chemistry.* Princeton, NJ: Princeton University Press.

[11] Jordan, A., S. Haidachera, G. Hanela, E. Hartungena, L. Marka, H. Seehausera, R. Schottkowskya, P. Sulzera, and T.D. Marka. 2009. "A high resolution and high sensitivity proton-transfer-reaction time-of-flight mass spectrometer (PTR-TOF-MS)." *International Journal of Mass Spectrometry* 286: 122128.

[12] Materic, Dusan, Mike Peacock, Matthew Kent, Sarah Cook, Vincent Gauci, Thomas Rockmann, and Rupert Holzinger. 2017. "Characterisation of the semi- volatile component of Dissolved Organic Matter by Thermal Desorption Proton Transfer Reaction Mass Spectrometry." *Scientific Reports* 7 (1): 15936.

[13] Myhre, G., D Shindell, F.-M. Breon, W. Collins, J. Fuglestvedt, J. Huang, D. Koch, et al. 2013. "Anthropogenic and Natural Radiative Forcing." In *Climate Change 2013: The Physical Science Basis. Contribution of Working Group I to the Fifth Assessment Report of the Intergovernmental Panel on Climate Change*, by T.F., D. Qin, G.-K. Plattner, M. Tignor, S.K. Allen, J. Boschung, A. Nauels, Y. Xia, V. Bex and P.M. Midgley Stocker. Cambridge: Cambridge University Press.

[14] Ramanathan, V., P. J. Crutzen, J. T. Kiehl, and D. Rosenfeld. 2001. "Aerosols, climate, and the hydrological cycle." *Science* 294 (no. 5549): 2119-2124.

[15] Ramaswamy, V., O. Boucher, J. Haigh, D. Hauglustine, J. Haywood, G. Myhre, and S. Solomon. 2001. "Radiative forcing of climate." 349.

[16] Stedmon, Colin A., Stiig Markager, and Rasmus Bro. 2003. "Tracing dissolved organic matter in aquatic environments using a new approach to fluorescence spectroscopy." *Marine Chemistry* 82 (3): 239-254.

[17] Warneke, C., J. Kuczynski, A. Hansel, A. Jordan, W. Vogel, and W. Lindinger. "Proton transfer reaction mass spectrometry (PTR-MS): propanol in human breath." *International journal of mass spectrometry and ion processes* 154, no. 1-2 (1996): 61-70.